Check for updates

Ultra-high capacity long-haul PDM-16-QAM-based WDM-FSO transmission system using coherent detection and digital signal processing

P. Sivakumar[1] · C. S. Boopathi[2] · M. G. Sumithra[3] · Mehtab Singh[4,5] · Jyoteesh Malhotra[4] · Amit Grover[6]

Abstract

The ever-increasing demand for wide channel bandwidth, high-speed information, and spectral-efficient communication links with advanced modulation schemes has led to the evolution of the free space optics (FSO) links. This paper proposes an FSO transmission link based on eight-channel wavelength division multiplexing technique integrating spectral-efficient polarization division multiplexing with a 16-level quadrature amplitude modulation (PDM-16-QAM) scheme, with each channel carrying 160 Gbps of information. The proposed link deploys coherent detection technique and the digital signal processing unit to boost the system efficiency and to compensate for the deterioration of the information signal due to channel fading, atmospheric attenuation and atmospheric turbulence. Using numerical simulations, we demonstrate an effective transmission of 1.28 Tbps data with FSO link range varying from 84 km to 1.95 km depending on the weather conditions with reasonable bit error rate results. We also scrutinize the output of the system with published works and demonstrate a better performance for the proposed FSO system i.e. bit rate and range. The proposed system can be implemented under complex atmospheric conditions to achieve a reliable high-speed transmission of information for fronthaul and backhaul links.

Keywords Free space optics (FSO) · Atmospheric attenuation · Quadrature amplitude modulation (QAM) · Bit error rate (BER) · Digital signal processing (DSP)

✉ Mehtab Singh
mehtab91singh@gmail.com

1 Department of EEE, PSG College of Technology, Coimbatore, India

2 Department of EEE, SRM University, Chennai, India

3 Department of BME, KPR Institute of Engineering and Technology, Coimbatore, India

4 Department of Engineering and Technology, Guru Nanak Dev University, Regional Campus, Jalandhar, India

5 Department of ECE, Satyam Institute of Engineering and Technology, (IKG-PTU, Kapurthala), Amritsar, India

6 Shaheed Bhagat Singh State Technical Campus, (IKG-PTU, Kapurthala), Ferozepur, India

1 Introduction

Free space optics (FSO) has become a viable option to conventional wireless communication technologies, as it uses the untapped and uncontrolled electromagnetic spectrum to provide safe information transmission with high-speed links (Singh and Kumar 2013). FSO technology offers an appealing and feasible solution for addressing the issue of spectrum congestion in wireless links based on conventional radio frequency (RF) spectrum (Khalighi and Uysal 2014). Other benefits of FSO links include secure transmission of information, low beam divergence, RF and electromagnetic interference immunity, low demand for mass and power, cost-effectiveness, wide channel bandwidth, last-mile access, etc. However, the output of FSO links is severely affected by the atmospheric attenuation provided by external weather conditions that degrade the quality of the optical beam that carries information and restricts the link distance. Another important factor that degrades FSO link efficiency is atmospheric turbulence, which results from fluctuations in atmospheric pressure and temperature along the path of signal propagation. It results in turbulence cells formation, which have different refractive indices and size. These turbulence cells act as a prism and result in the destructive or constructive interference of the optical beam, which carries information. This result in spontaneous phase fluctuations and the information signal amplitude variations at the receiver terminal, also known as the scintillation effect.

Recently, much work has been published on improving the efficiency of FSO links. The work in (Badar et al. 2018) describes the performance analysis of FSO link based on 8-wavelength division multiplexed (WDM) channels each transmitting 10 Gbps differential phase-shift keyed (DPSK) signals over a 3-km range under different climate conditions. The efficiency of WDM-FSO link under different weather affairs by incorporating polarization-shift keying (PolSK) was exhibited in Jeyaseelan et al. (2018a, b). The performance of FSO link using orthogonal frequency division multiplexing (OFDM) over 185 km distance with an optical semiconductor amplifier has been discussed in (Chaudhary et al. 2014). The integration of polarization division multiplexing (PDM) in a high-speed FSO link with OFDM and coherent detection was examined for various weather affairs in (Kaur et al. 2019). Here (Prabu et al. 2017) reports the efficacy of a 6.24 Gbps FSO link based on a spectrum sliced WDM technique (SS-WDM). In Chaudhary and Amphawan (2018a, b) the performance improvement of the FSO link was reported using mode division multiplexing (MDM) to transmit 7.5 Gbps of information in different weather conditions. The combination of OFDM along with MDM-WDM hybrid scheme was reported in Amphawan et al. (2019) to attain an 80 Gbps FSO link over a distance of 50 km. Multi-access optical code division multiplexing (OCDMA) with spectral amplitude coding (SAC) and MDM was incorporated in an 8 km FSO link in Sarangal et al. (2017). Performance assessment of wavelength diversity and time diversity based FSO link under the influence of Gamma–Gamma distribution and log-normal distribution conditions deploying hybrid pulse position modulation with binary phase shift keying and subcarrier intensity modulation has been reported in Sharma and Grewal (2020). The development of a hybrid FSO/RF transmission link incorporating technique for optimal selection of threshold levels for improved link performance is discussed in Shrivastava et al. (2020). The authors in Algamal et al. (2020) have reported a reliable FSO transmission link capable of catering to the multi-level end user needs under Egypt climate conditions. The proposed link performance has been investigated for different sandstorm conditions and pointing error angles.

The demand for transmission of high-speed data and spectral-efficient performance has led to a strong interest in advanced modulation systems-based FSO links. Techniques

like multi-level quadrature amplitude modulation (QAM), phase shift keying (PSK) and OFDM with coherent detection can be incorporated in future wireless systems using FSO links with a 100 G-bit rate. These techniques of modulation transmitting k-bits per symbol achieve a k-bits/sec/Hz/polarization spectral efficiency compared with 1-bit/sec/Hz/polarization efficiency of binary modulation schemes (Makovejs et al. 2010; Mori et al. 2009). Here Charlet et al. (2009) reports 112 Gbps of information transmitted through a single-channel using QPSK signals and a WDM-based optical fiber link. The application of 16-QAM signals has been reported in Renaudier et al. (2009) along with signal amplification using different amplifiers for achieving 112 Gbps-1022 km WDM-based optical fiber communication. 16-QAM signals for the transmission along 240 km of single-mode fiber link with high-speed data using EDFA has been demonstrated in Winzer et al. (2010). The single-channel and dual-polarized, secure FSO link performance comparison employing 16-QAM signals was addressed in Jain and Mehra (2017). In order to mitigate phase mismatch losses and to retrieve high-speed data, digital signal processing (DSP) algorithms deployed at the receiver was reported in Zhou and Yu (2009) and Zhong et al. (2018). The work in Tsukamoto et al. (2006) demonstrates the use of DSP and homodyne detection in a 20 Gbps optical fiber link employing QPSK signals. By integrating the state of the art modulation schemes with coherent detection and DSP algorithms, FSO links can be explored for high-speed applications.

In this paper, we report an eight-channel WDM-FSO link based on PDM-16-QAM scheme. The principal motivation behind the work is: (1) to realize a high-capacity WDM-based long-range FSO link by using spectral-efficient PDM-16-QAM scheme, (2) improving the performance of the link by the integration of coherent detection and DSP, (3) investigating the impact of air turbulence and weather on the proposed FSO link. The remaining paper is divided as follows: Sect. 2 deals with M-QAM modulation performance analysis. The schematics for the proposed system are discussed in Sect. 3. The channel modelling and the link parameters employed in this study are defined in Sect. 4. Section 5 reports the results of the investigation of the proposed FSO link and a comparison of its performance with published works. Conclusion to this study is given in Sect. 6.

2 M-QAM scheme symbol error rate (SER) investigation

Assessment of modulation schemes of higher-order can be carried out by computing SER across a spectrum of background noise specified as E_s/N_o (power/bit to noise density ratio) (Raju and Reddy 2016). SER is expressed mathematically for the M-QAM scheme as (Sklar 2001):

$$SER = 2\left(1 - \frac{1}{M}\right)erfc\left(\sqrt{\frac{3}{2(M-1)}\frac{E_s}{N_0}}\right) + \left(1 - \frac{2}{\sqrt{M}} + \frac{1}{M}\right)erfc^2\left(\sqrt{\frac{3}{2(M-1)}\frac{E_s}{N_0}}\right)$$
(1)

We test the M-QAM scheme for SER versus E_s/N_o and compare simulated results with analytical plots, as illustrated in the Fig. 1. The findings show that SER is also increased by the increase in the value of M and the analytical plots agree with the simulation results. The best output is observed for 16-QAM and therefore the proposed system employs 16-QAM modulation scheme.
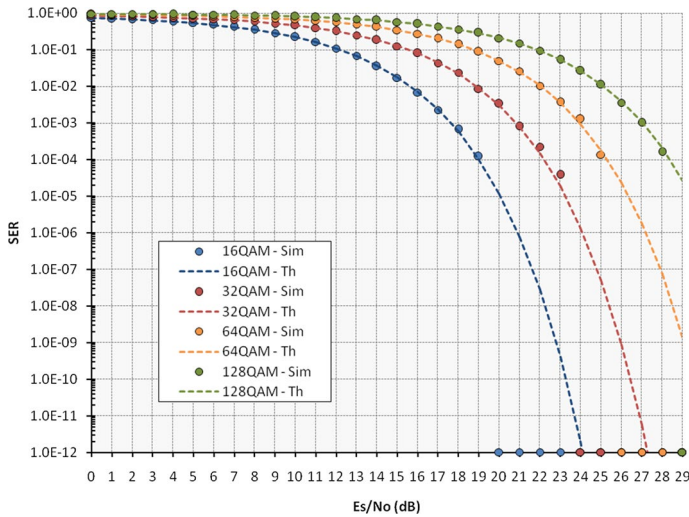
Fig. 1 SER versus E_s/N_o

3 Proposed FSO link design

Figure 2 demonstrates the eight-channel WDM-FSO transmission link schematic with PDM-16-QAM signals developed using Optisystem tool. Figure 3a, b show schematic of transmitter and receiver sections for PDM-16-QAM signals.

Eight distinct frequency channels (193.1–193.8 THz) with channel spacing of 100 GHz are used in the proposed system, where each channel transmits 160 Gbps of information to create a 1.28 Tbps WDM-FSO transmission link. The PDM-16-QAM signal is generated by using a
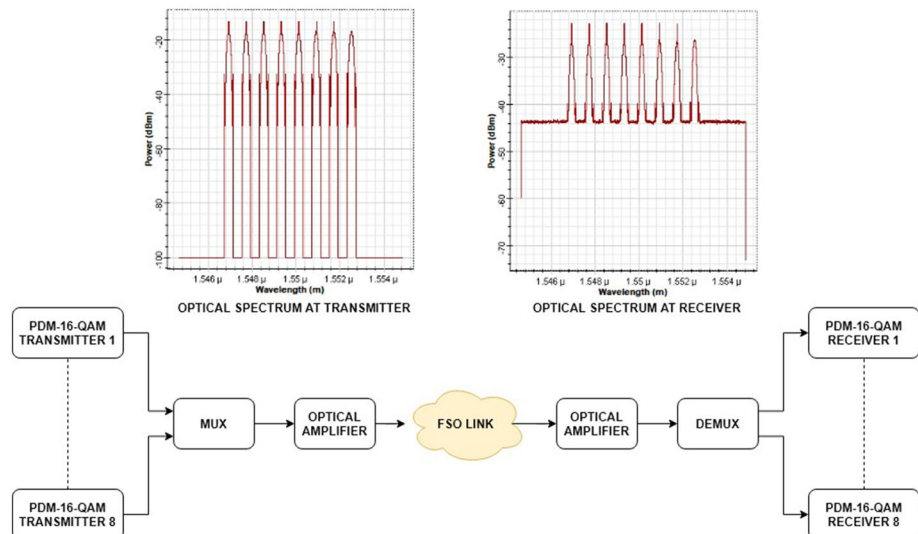

Fig. 2 Schematic of the proposed WDM-FSO transmission link using the PDM-16-QAM signals
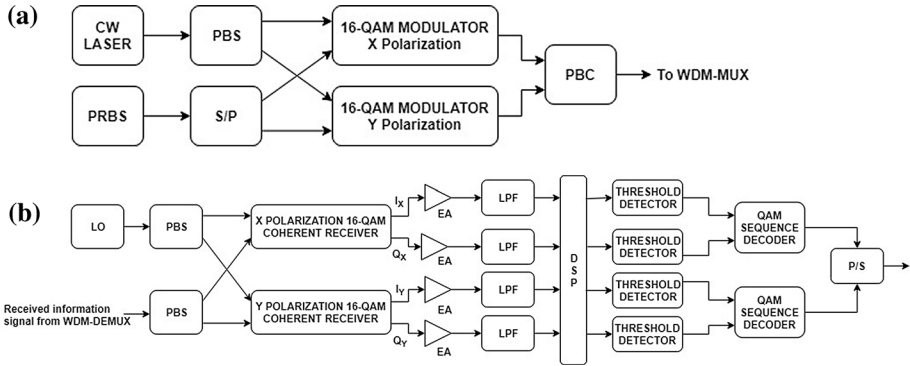
Fig. 3 Schematic of PDM-16-QAM. **a** Transmitter section. **b** Receiver section

continuous wave laser with a 0.1 MHz line width as depicted in Fig. 3a. PBS with a 45^0 device angle divides the optical beam into two orthogonal polarized beams. An information stream of 160 Gbps is generated using a pseudo-random bit sequence (PRBS) generator. Each data stream is modulated by a 16-QAM modulator over a distinct polarized laser beam. The information signal is then multiplexed from each section of the PDM-16-QAM transmitter using a MUX.

The received signal is amplified with a flat gain EDFA at the receiver terminal, followed by a WDM DEMUX separating independent frequency channels and directing them to separate PDM-16-QAM receivers. Each receiver unit uses a local oscillator (LO) and a PBS to detect the polarized information signal as depicted in Fig. 3b. The in-phase and quadrature-phase electrical signals of the orthogonal polarization states are amplified with an electrical amplifier (EA) with a gain of 20 dB and a noise power of -100 dBm, followed by a low pass (LPF). Figure 4 illustrates various DSP-related steps.

Different steps are: (1) A 4th order Bessel filter is used for filtering noise power, (2) Cubic interpolation is implemented for resampling, (3) Quadrature imbalance (QI) correction is performed to reduce the amplitude and the phase imbalance in the symbol, (4) Adaptive equalization for demultiplexing the orthogonal polarized beams. At the DSP receiver, the input signal is expressed as (Ciblat and Vandendorpe 2003):

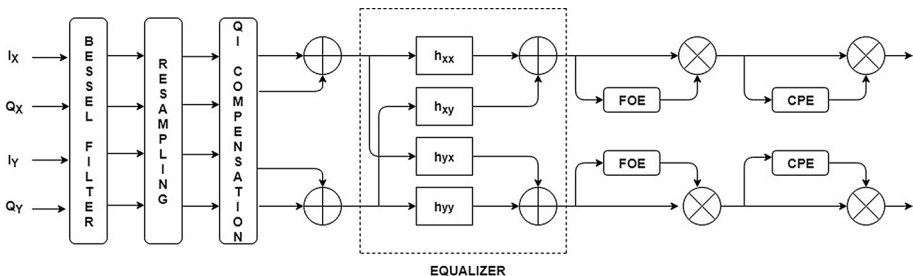$$S(k) = C(k) \cdot e^{j \cdot \left(2\pi \Delta f k T + \varphi_k\right)} + n(k) \tag{2}$$

Fig. 4 Various steps in DSP module

where $C(k)$ denotes data symbols, Δf denotes carrier frequency offset, φ_k is carrier phase, T is time period, and $n(k)$ denotes a Gaussian random variable. The expression of the fourth power of the received information signal is given as (Ciblat and Vandendorpe 2003):

$$S^4(k) = \frac{1}{4} arg\{\max[|Z(f)|]\} \tag{3}$$

where

$$|Z(f)| = \frac{1}{N} \sum_{k=0}^{N-1} S^4(k) \cdot e^{-j \cdot (2\pi fkT)} \tag{4}$$

where N indicates block length, (5) Frequency offset estimation (FOE) is deployed to eliminate the mismatch between the frequency of transmitting laser and local oscillator, (6) Blind phase search algorithm is used for carrier phase estimation (CPE) to mitigate the mismatch between the transmitted signal phase and the local carrier signal phase. The information signal $Z(f)$ is rotated by the phase angles (φ_b) which are expressed as (Zhou et al. 2014):

$$\varphi_b = \frac{b}{B} \cdot \frac{\pi}{2} - \frac{\pi}{4} \quad \text{where } b \in \{0, 1, 2, \ldots\ldots, B-1\} \tag{5}$$

A decision circuit is deployed for estimating the distance $|d_{k,b}|^2$ to the nearest constellation symbol in the complex plane, which is calculated by:

$$|d_{k,b}|^2 = \left|Z_k e^{j\varphi_b} - \hat{X}_{k,b}\right|^2 \tag{6}$$

where $\hat{X}_{k,b}$ denotes the decision of $Z_k e^{j\varphi_b}$. The signal is decoded with a QAM decoder and the information is retrieved at the output of parallel to serial converter.

4 Channel modelling

In this study, using the proposed system, 1.28 Tbps of information is transmitted over the free space under the effect of various atmospheric conditions. The FSO link can be defined in mathematical terms as (Singh and Malhotra 2019):

$$P_{Received} = P_{Transmitted}\left(\frac{d_R^2}{(d_T + \theta Z)^2}\right)10^{-\sigma Z/10} \tag{7}$$

where d_R is the aperture diameter of the receiver (m), d_T is the aperture diameter of the transmitter (m), θ is beam divergence angle (mrad), Z is distance/range (km) and σ is attenuation coefficient (dB/km). The FSO link quality depends on external weather, which degrade the signal quality and reduce the power received. Under different conditions of fog/haze, the attenuation coefficient value can be calculated mathematically as (Kim et al. 2006):

$$\beta_{fog/haze}(\lambda) = \frac{3.91}{V}\left(\frac{\lambda}{550}\right)^{-p} \tag{8}$$

where $V(km)$ represents visibility, $\lambda(nm)$ represents operating wavelength, and p represents the size distribution scattering coefficient which can be found by using Kim model as (Kim et al. 2006):

$$p = \begin{cases} 1.6 & V > 50 \\ 1.3 & 6 < V < 50 \\ 0.16V + 0.34 & 1 < V < 6 \\ V - 0.5 & 0.5 < V < 1 \\ 0 & V < 0.5 \end{cases} \tag{9}$$

On the other hand, due to rainfall conditions the attenuation coefficient value is independent of the operating wavelength and depends on the rainfall intensity. Under rainfall conditions, the attenuation coefficient is given as (Mohammad 2014):

$$\beta_{rain} = 1.076 R^{0.67} \tag{10}$$

where R (mm/hr) indicates the rainfall rate. The attenuation because of rainfall conditions can be approximated for FSO links, using the formula:

$$\alpha_{rain} = \frac{2.8}{V} \tag{11}$$

where V (km) represents visibility range, which is dependent upon rainfall rate as summarized in Table 1.

Another important factor limiting the efficiency of the FSO links is atmospheric turbulence, which leads to random phase and signal strength variations at receiver terminal. Gamma–Gamma (GG) turbulence model is considered in this work because it is capable of accurately modeling weak to strong turbulence regimes (Djordjevic et al. 2007; Anguita et al. 2005). The GG channel probability density function is defined in mathematical terms as:

$$f(I) = \frac{2(\alpha\beta)^{(\alpha+\beta)/2}}{\Gamma(\alpha)\Gamma(\beta)} I^{[(\alpha+\beta)/2]-1} K_{\alpha-\beta}\left(2\sqrt{\alpha\beta I}\right) \tag{12}$$

where α and β denote large and small scale effects of turbulence, which are mathematically described in Eqs. (13) and (14) respectively, Γ represents the gamma function, $K(.)$ denotes second-order Bessel function.

$$\alpha = \left\{ \exp\left[\frac{0.49\sigma^2}{\left(1 + 1.1\sigma^{12/5}\right)^{7/6}}\right] - 1 \right\}^{-1} \tag{13}$$

Table 1 Visibility range and rainfall rates (Grover and Sheetal 2019)

Rainfall type	Rate of Rainfall R (mm/hr)	Visibility V (km)
Heavy	25	1.9–2
Medium	12.5	2.8–40
Light	0.25	18–20

Table 2 Parameters values (Chaudhary and Amphawan 2018; Amphawan et al. 2019; Sarangal et al. 2017)

Parameter	Value
Number of frequency channels	8
Channel spacing	100 GHz
Operating frequency	193.1–193.8 THz
Transmission power/channel	10 dBm
PIN photodetector dark current	10 nA
Aperture diameter	10 cm
EDFA gain	20 dB
MZM extinction ratio	30 dB
Symbol rate	20 Gbps
Bit rate/channel	160 Gbps
Laser linewidth	0.1 MHz
Number of samples	65,536
Beam divergence	0.25 mrad

Table 3 Attenuation coefficient (Chaudhary et al. 2014; Chaudhary and Amphawan 2018a, b; Amphawan et al. 2019; Sarangal et al. 2017)

Weather	Attenuation (dB/km)
Heavy Haze	10.15
Mild Haze	4.285
Low Haze	1.537
Clear	0.14
Heavy Fog	22
Thick Fog	16
Thin Fog	9
Heavy Rain	19.28
Medium Rain	9.64
Light Rain	6.27

$$\beta = \left\{ \exp\left[\frac{0.51\sigma^2}{\left(1 + 0.69\sigma^{12/5}\right)^{5/6}} \right] - 1 \right\}^{-1} \tag{14}$$

where $\sigma^2 = 1.23 C_n^2 k^{\frac{7}{6}} Z^{\frac{11}{6}}$ denotes Roytov variance, Z is the link distance, $k = 2\pi/\lambda$ is the optical wave number, λ is the operating wavelength, and C_n^2 denotes the refractive index structure parameter. Table 2 describes the parameter values used in the analysis. The attenuation values are mentioned in Table 3. For various atmospheric turbulence conditions, the refractive index structure parameter values are mentioned in Table 4.

We also take the impact of geometric loss/beam divergence into consideration in this work while investigating the performance of the proposed link. As the optical beam carrying information signal propagates through free space, it spreads out due to diffraction. As a result, a portion of the transmitted optical beam is not received at the aperture of the receiver antenna resulting in geometric loss L_G that can be measured as (Al-Gailani et al. 2013):

Table 4 Refractive index structure parameter for different atmospheric turbulence conditions

Turbulence condition	Refractive index structure parameter C_n^2
Strong	5×10^{-13} m$^{-2/3}$
Moderate	5×10^{-15} m$^{-2/3}$
Weak	5×10^{-17} m$^{-2/3}$

$$L_G(Geometric\ loss) = -20 \log \left[\frac{d_R}{(d_T + \theta Z)^2} \right] \tag{15}$$

where d_R and d_T represent receiver and transmitter antenna aperture diameter (m) respectively, Z represents the link range (km), θ represents the beam divergence angle (*mrad*). Figure 5 reports the geometric loss/beam divergence loss with FSO transmission range.

5 Results and discussion

Figure 6 reports the bit error rate (BER) versus the FSO transmission range under clear weather conditions. It can be observed from the results that the system BER degrades with increasing FSO transmission range. Furthermore, as the transmission range is increased, the constellation symbols of the received information signal becomes more deteriorated, rendering it difficult for the demodulator units to detect the information signal satisfactorily. The maximum feasible transmission range with an appropriate log of BER (− 2.42 i.e. the FEC limit Karaki et al. 2013) for the proposed system is computed as 84 km under clear weather conditions.

Figure 7 reports the error vector magnitude (EVM) and the power plots obtained against the FSO transmission range using the proposed link under clear conditions. EVM is a performance metric used to measure the demodulator unit output performance in the presence of channel noise and is derived from the obtained signal constellation diagram. From

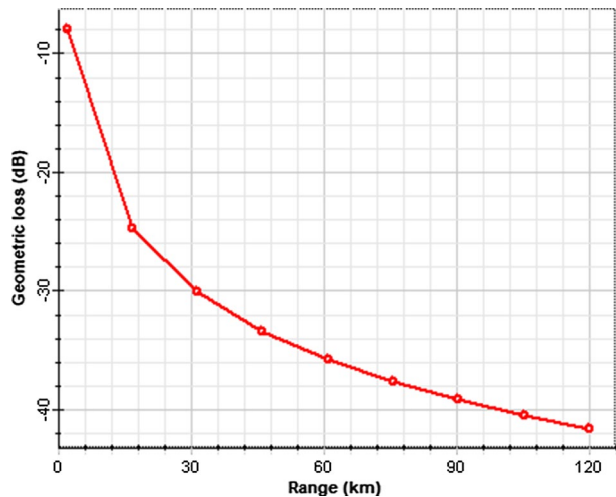**Fig. 5** Geometric loss/beam divergence loss versus FSO transmission range

Fig. 6 Log of BER versus transmission range in clear weather
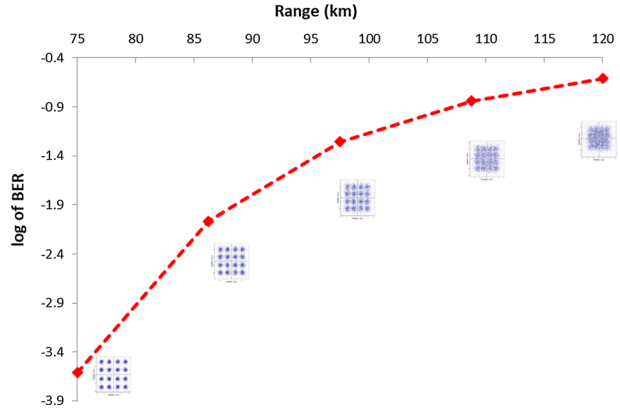

Fig. 7 EVM % and power versus transmission range in clear weather
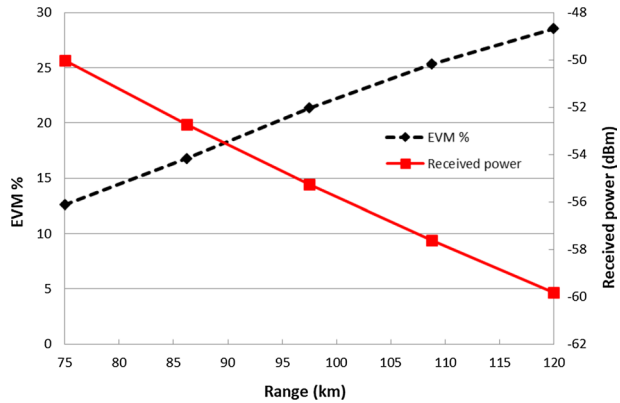

Fig. 7, it is seen that as the transmission range increases, the percentage of EVM increases and the power received decreases, making it difficult for the demodulator to accurately recover the information from the received signal.

Figure 8 reports the electrical signal at the transmitter terminal and the receiver terminal under clear weather conditions in the proposed 1.28 Tbps 84 km FSO transmission. The overall similarity of the transmitted and received electrical signal indicates an effective transmission of 1.28 Tbps of information over 84 km FSO link range under clear weather conditions. Figure 9 shows the data signal constellation graphs at various points in the link.

In this work, we also investigate the proposed WDM-FSO transmission system under different conditions of haze, rain, and fog. Figure 10 reports BER of received signal versus transmission range, using the proposed link, under different weather conditions. From Fig. 10a, the maximum transmission range under low haze with an acceptable BER is 16.7 km which reduces to 7.5 km for mild haze and 3.7 km for heavy haze. Likewise, from Fig. 10b the range is 5.55 km, 3.9 km, and 2.15 km, respectively under heavy, medium, and light rain. Figure 10c demonstrate successful transmission of 1.28 Tbps of information over 4.1 km FSO range under thin fog conditions, decreasing to 2.55 km under thick fog and 1.95 km under heavy fog. The results presented show that as the atmospheric attenuation increases, the overall transmission range with good BER decreases.

Fig. 8 Electrical signal at **a** transmitter terminal **b** receiver terminal
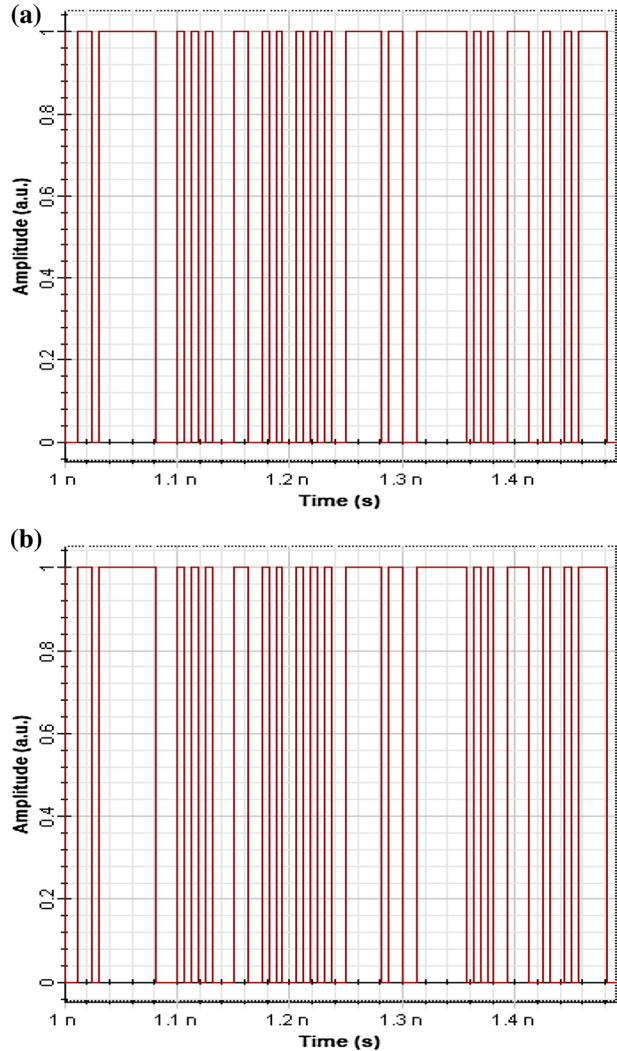
In addition, the proposed FSO link is scrutinized under the influence of varying atmospheric turbulence conditions. Figure 11 reports the BER plots of the received signal versus refractive index structure parameter at varying range and weather conditions. From Fig. 11 it is observed that as the refractive index structure parameter increases from weak turbulence $\left(C_n^2 = 5 \times 10^{-17}\right)$ to strong turbulence $(C_n^2 = 5 \times 10^{-13})$, the system BER under all weather conditions degrades. It can also be observed that the degrading effect of increasing atmospheric turbulence on the proposed system BER is significantly higher at longer link distances. This is because the size of the information-carrying optical beam at longer distances is relatively large, leading to higher phase distortions.

Furthermore, in Table 5 we compare the transmission performance of the proposed 1.28 Tbps WDM-FSO transmission system with previously published works (Badar et al. 2018; Jeyaseelan et al. 2018a, b; Chaudhary et al. 2014; Kaur et al. 2019; Prabu
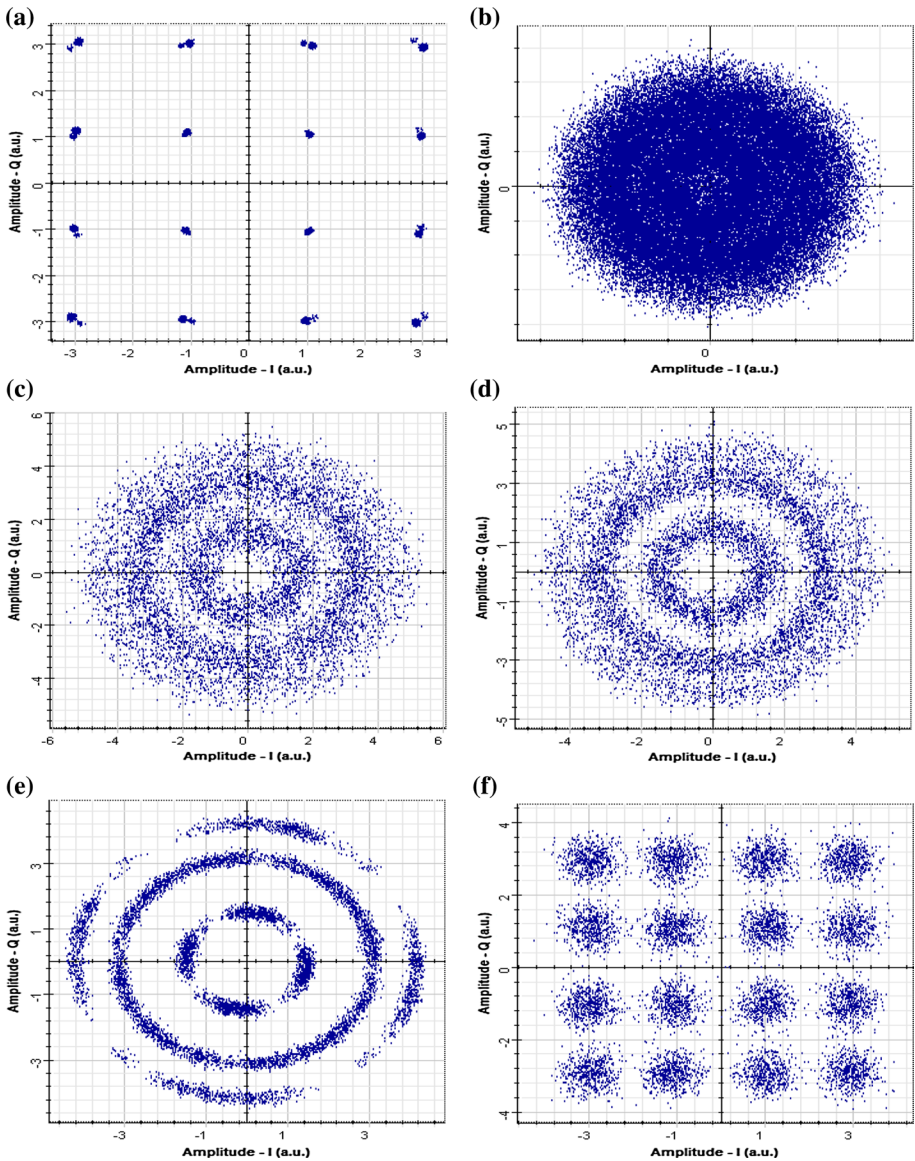
Fig. 9 Constellation graph **a** at transmitter **b** at receiver **c** after QI compensation **d** after adaptive equalization **e** after FOE **f** after CPE

et al. 2017; Chaudhary and Amphawan 2018a, b; Amphawan et al. 2019; Sarangal et al. 2017). The results show that the proposed FSO system has a higher merit i.e. bit rate and range compared to previous works by incorporating PDM and advanced higher-order modulation scheme with coherent detection and DSP for free space loss compensation and carrier phase estimation at the receiver terminal.

Fig. 10 log of BER versus range for **a** haze **b** rain and **c** fog conditions
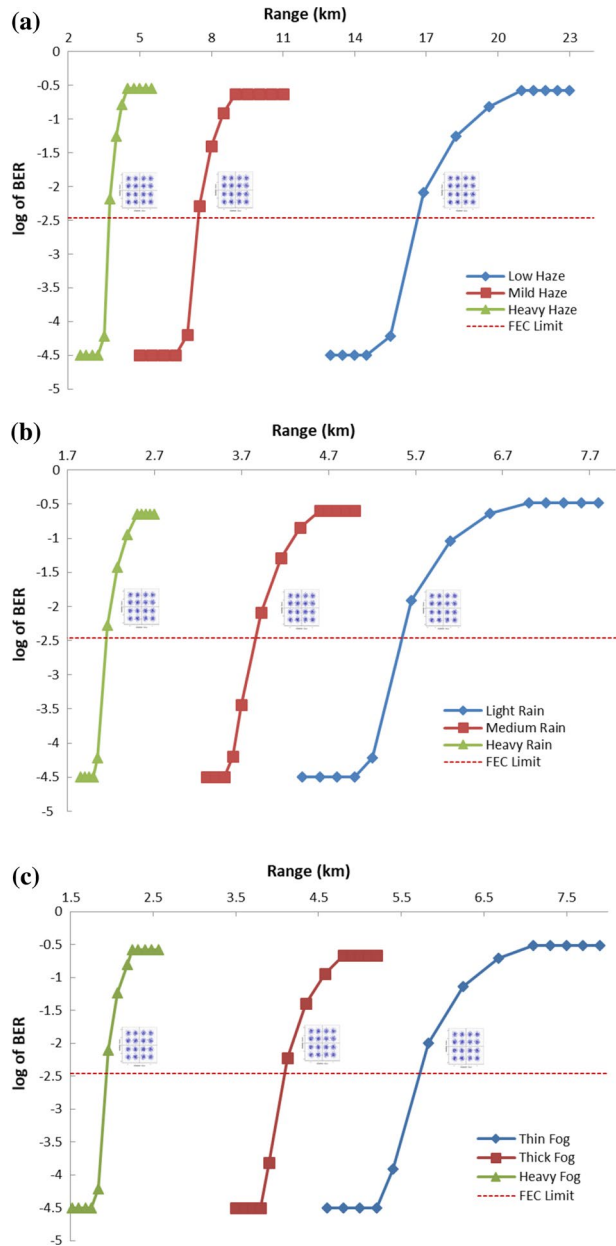
6 Conclusion

In this study, a 8 $\lambda\times$ 160 Gbps WDM-FSO transmission link based on PDM-16-QAM scheme using coherent detection and DSP for free space loss compensation and carrier phase estimation at the receiver terminal is proposed. The performance for various

Fig. 11 Log of BER versus refractive index structure under **a** haze **b** rain **c** fog conditions
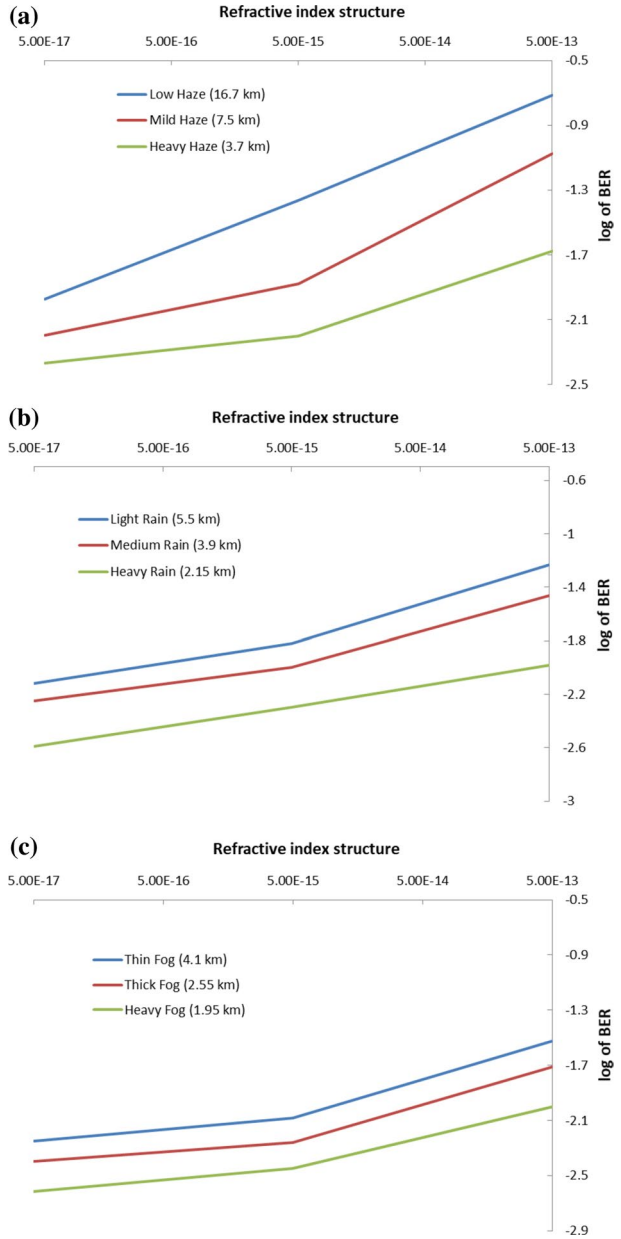
weather conditions and atmospheric turbulence has also been investigated. The findings reported show that in clear weather, 1.28 Tbps of information is transmitted successfully over 84 km of FSO link range, which for heavy fog reduces to 1.95 km. The proposed system provides a suitable technique for realizing effective high-speed data

Table 5 Comparison of proposed FSO system with previous works

Method	Bit rate	Weather conditions	Range (km)
WDM based FSO link with RZ–DPSK modulation scheme Badar et al. (2018)	8 λ× 10 Gbps	Clear	3
		Low Haze	3
		Thin Fog	1.2
		Thick Fog	0.5
WDM based FSO link with PolSK modulation scheme Jeyaseelan et al. (2018a, b)	4 λ× 2.5 Gbps	Clear	275
		Light Rain	25.9
		Moderate Rain	21.4
		Heavy Rain	15.3
		Low Fog	7.1
		Heavy Fog	5.8
OFDM based FSO link with SOA pre-amplification Chaudhary et al. (2014)	10 Gbps	Clear	185
		Heavy fog	2.5
Hybrid CO-OFDM-PDM based FSO link Kaur et al. (2019)	2 states of polarization (X and Y) × 2 Gbps	Clear	5
		Fog	2
SS-WDM based FSO link Prabu et al. (2017)	4 λ× 1.56 Gbps	Clear	140
		Light Haze	66
		Heavy Haze	19
		Light Rain	8.3
		Moderate Rain	5.7
		Heavy Rain	3.14
		Light Fog	3.8
		Heavy Fog	2.5

Table 5 (continued)

Method	Bit rate	Weather conditions	Range (km)
MDM based FSO link with NRZ modulation scheme Chaudhary and Amphawan (2018a, b)	3 spatial modes × 2.5 Gbps	Clear	2.5
		Thin Fog	0.6
		Thick Fog	0.4
		Heavy Fog	0.2
Hybrid OFDM-WDM-MDM based FSO link with 4-QAM modulation Amphawan et al. (2019)	2 λ × 2 spatial modes × 20 Gbps	Clear	50
		Thin Fog	4
		Thick Fog	3
		Heavy Fog	2
Hybrid SAC-OCDMA-MDM based FSO link Sarangal et al. (2017)	10 × 10 Gbps	Clear	8
		Thin Fog	1.5
		Thick Fog	1.25
		Heavy Fog	1
Proposed system	8 λ × 160 Gbps (1.28 Tbps)	Clear	84
		Low Haze	16.7
		Mild Haze	7.5
		Heavy Haze	3.7
		Light Rain	5.55
		Moderate Rain	3.9
		Heavy Rain	2.15
		Thin Fog	4.1
		Thick Fog	2.55
		Heavy Fog	1.95

transmission under complex atmospheric conditions for the future-generation communication networks.

References

Al-Gailani, S.A., Mohammad, A.B., Shaddad, R.Q.: Enhancement of free space optical link in heavy rain attenuation using multiple beam concept. Optik **124**(21), 4798–4801 (2013)

Algamal, A.A., Fayed, H.A., Mahmoud, M., et al.: Reliable FSO system performance matching multi-level customer needs in Alexandria City, Egypt, climate: sandstorm impact with pointing error. Opt. Quant. Electron. **52**, 349 (2020)

Amphawan, A., Chaudhary, S., Chan, V.: Optical millimeter wave mode division multiplexing of LG and G modes for OFDM Ro-FSO system. Opt. Commun. **431**, 245–254 (2019)

Anguita, J.A., Djordjevic, I.B., Neifeld, M.A., Vasic, B.V.: High-rate error-correction codes for the optical atmospheric channel. In: Proceedings of the SPIE, free-space laser communications, 58920 V (2005)

Badar, N., Jha, R., Towfeeq, I.: Performance analysis of 80 (8 × 10) Gbps RZ-DPSK based WDM-FSO system under combined effects of various weather conditions and atmospheric turbulence induced fading employing Gamma-Gamma fading model. Opt. Quant. Electron. **50**, 1–11 (2018)

Charlet, G., Renaudier, J., Mardoyan, H., Tran, P., Pardo, O.B., Verluise, F., Achouche, M., Boutin, A., Blache, F., Dupuy, J.-Y., Bigo, S.: Transmission of 164-Tbit/s capacity over 2550 km using PDM QPSK modulation format and coherent detection. J. Lightwave Technol. **27**(3), 153–157 (2009)

Chaudhary, S., Amphawan, A.: Selective excitation of LG 00, LG 01, and LG 02 modes by a solid core PCF based mode selector in MDM-Ro-FSO transmission systems. Laser Phys. **28**(7), 1–8 (2018b)

Chaudhary, S., Amphawan, A.: Solid core PCF-based mode selector for MDM-Ro-FSO transmission systems. Photon. Link Commun. **36**(2), 263–271 (2018a)

Chaudhary, S., Amphawan, A., Nisar, K.: Realization of free space optics with OFDM under atmospheric turbulence. Optik **125**(18), 5196–5198 (2014)

Ciblat, P., Vandendorpe, L.: Blind carrier frequency offset estimation for noncircular constellation-based transmissions. IEEE Trans. Signal Process. **51**, 1378–1389 (2003)

Djordjevic, I.B., Vasic, B., Neifeld, M.A.: LDPC coded OFDM over the atmospheric turbulence channel. Opt. Express **15**, 6336–6350 (2007)

Grover, A., Sheetal, A.: Improved performance investigation of 10 Gb/s–10 GHz 4-QAM Based OFDM-Ro-FSO transmission link. J. Opt. Commun. (published online ahead of print 2019)

Jain, D., Mehra, R.: Performance of 120 Gbps single and dual polarized 16-QAM coherent FSO systems under various turbulence regimes. International Conference on Computing and Communication Technologies for Smart Nation (IC3TSN), Gurgaon (2017), pp. 89–94

Jeyaseelan, J., Kumar, S., Caroline, B.: PolSK and ASK modulation techniques based BER analysis of WDM-FSO system for under turbulence conditions. Wireless Pers. Commun. **103**(4), 3221–3237 (2018a)

Jeyaseelan, J., Kumar, S., Caroline, B.: Performance analysis of free space optical communication system employinh WDM-PolSK under turbulent weather conditions. J. Optoelectron. Adv. Mater. **20**(9), 506–514 (2018b)

Karaki, J., Giacoumidis, E., Grot, D., Guillossou, T., Gosset, C., Le Bidan, R., Le Gall, T., Jaouën, Y., Pincemin, E.: Dual-polarization multi-band OFDM versus single-carrier DPQPSK for 100 Gb/s long-haul WDM transmission over legacy infrastructure. Opt. Express **21**, 16982 (2013)

Kaur, G., Srivastava, D., Singh, P., Parasher, Y.: Development of a novel hybrid PDM/OFDM technique for FSO system and its performance analysis. Opt. Laser Technol. **109**, 256–262 (2019)

Khalighi, M.A., Uysal, M.: Survey on free space optical communication: a communication theory perspective. IEEE Commun. Surv. Tutor. **16**(4), 2231–2258 (2014)

Kim, I., Mcarthur, B., Korevaar, E.: Comparison of laser beam propagation at 785 and 1550 nm in fog and haze for optical wireless communications. Proc SPIE optical wireless communication **6303**, 1 (2006)

M. Raju and K. A. Reddy (2016) Evaluation of BER for AWGN, Rayleigh fading channels under M-QAM modulation scheme. In: *International conference on electrical, electronics, and optimization techniques (ICEEOT), Chennai*, pp. 3081–3086 (2016)

Makovejs, S., Millar, D.S., Mikhailov, V., Gavioli, G., Killey, R.I., Savory, S.J., Bayvel, P.: Novel method of generating QAM-16 signals at 213 Gbaud and transmission over 480 km. IEEE Photon. Technol. Lett. **22**(1), 36–38 (2010)

Mohammad, A.B.: Optimization of FSO system in tropical weather using multiple beams. In: *IEEE 5th International Conference on Photonics (ICP), Kuala Lumpur*, pp. 109–112 (2014)

Mori, Y., Zhang, C., Igarashi, K., Katoh, K., Kikuchi, K.: Unrepeated 200-km transmission of 40-Gbit/s 16-QAM signals using digital coherent receiver. Opt. Express **17**(3), 1435–1441 (2009)

Prabu, K., Charanya, S., Jain, M., Guha, D.: BER analysis of SS-WDM based FSO system for Vellore weather conditions. Opt. Commun. **403**, 73–80 (2017)

Renaudier, J., Charlet, G., Bertran-Pardo, O., Mardoyan, H., Tran, P., Salsi, M., Bigo, S.: Transmission of 100 Gb/s coherent PDM-QPSK over 16 x 100 km of standard fiber with allerbium amplifiers. Opt. Express **17**(7), 5112–5119 (2009)

Sarangal, H., Singh, A., Malhotra, J., Chaudhary, S.: A cost effective 100Gbps hybrid MDM-OCDMA-FSO transmission system under atmospheric turbulences. Opt. Quant. Electron. **49**, 184 (2017)

Sharma, K., Grewal, S.: Performance assessment of hybrid PPM–BPSK–SIM based FSO communication system using time and wavelength diversity under variant atmospheric turbulence. Opt. Quant. Electron. **52**, 430 (2020)

Shrivastava, S., Sengar, S., Singh, S., et al.: Threshold optimization for modified switching scheme of hybrid FSO/RF system in the presence of strong atmospheric turbulence. Photon. Link Commun. **40**, 103–113 (2020)

Singh, J., Kumar, N.: Performance analysis of different modulation format on free space optical communication system. Optik Int. J. Light Electron. Opt. **124**(20), 4651–4654 (2013)

Singh, M., Malhotra, J.: Performance comparison of high-speed long-reach mode division multiplexing-based radio over free space optics transmission system using different modulation formats under the effect of atmospheric turbulence. Opt. Eng. **58**(4), 046112 (2019)

Sklar, B.: Digital Communications: Fundamentals and Applications. Prentice Hall, New York (2001)

Tsukamoto, S., Katoh, K., Kikuchi, K.: Unrepeated 20-Gbit/s QPSK transmission over standard single-mode fiber using homodyne detection and digital signal processing for dispersion compensation. In: *Optical Fiber Communication Conference and the National Fiber Optic Engineers Conference, Anaheim, CA* (2006)

Winzer, P.J., Gnauck, A.H., Doerr, C.R., Magarini, M., Buhl, L.L.: Spectrally efficient long-haul optical linking using 112-Gb/s polarization-multiplexed 16-QAM. J. Lightwave Technol. **28**(4), 547–556 (2010)

Zhong, K., Zhou, X., Huo, J., Yu, C., Lu, C., Lau, A.P.T.: Digital signal processing for short-reach optical communications: a review of current technologies and future trends. J. Lightw. Technol. **36**(2), 377–400 (2018)

Zhou, X., Zhong, K., Gao, Y., Lu, C., Lau, A.P.T., Long, K.: Modulation-format-independent blind phase search algorithm for coherent optical square M-QAM systems. Opt. Express **22**, 24044–24054 (2014)

Zhou, X., Yu, J.: Digital signal processing for coherent optical communication. In: 18th Annual Wireless and Optical Communications Conference, Newark, NJ, pp. 1–5 (2009)